View metadata, citation and similar papers at core.ac.uk

brought to you by CORE

provided by NASA Technical Reports Server

303115

N95-10569

CASE STUDY OF A LOW-REFLECTIVITY PULSATING MICROBURST: NUMERICAL SIMULATION OF THE DENVER, 8 JULY 1989, STORM

Fred H. Proctor

Flight Management Division
NASA Langley Research Center
Hampton, VA 23681-0001

1. INTRODUCTION

On 8 July 1989, a very strong microburst was detected by the Low-Level Windshear Alert System (LLWAS), within the approach corridor just north of Denver Stapleton Airport. The microburst was encountered by a Boeing 737-200 in a "go-around" configuration which was reported to have lost considerable air speed and altitude during penetration (Wilson et al. 1991; Hughes 1990). Data from LLWAS revealed a pulsating microburst with an estimated peak velocity change of 48 m/s. Wilson et al. (1991) reported that the microburst was accompanied by no apparent visible clues such as rain or virga, although blowing dust was present. Weather service hourly reports indicated virga in all quadrants near the time of the event. A National Center for Atmospheric Research (NCAR) research Doppler radar was operating; but according to Wilson et al., meaningful velocity could not be measured within the microburst due to low radar-reflectivity factor and poor siting for windshear detection at Stapleton.

This paper presents results from the three-dimensional numerical simulation of this event, using the Terminal Area Simulation System (TASS) model (Proctor 1987). The TASS model is a three-dimensional nonhydrostatic cloud model that includes parameterizations for both liquid- and ice-phase microphysics, and has been used in investigations of both wet- and dry-microburst case studies (e.g., Proctor 1988, 1992; Proctor and Bowles 1992). The focus of this paper is the pulsating characteristic and the very-low radar reflectivity of this event.

2. MICROBURST PULSING

Microburst events commonly exhibit pulsating variations as indicated by secondary increases in low-level wind speed and horizontal velocity change (e.g., Hjelmfelt 1988; Cornman et al. 1989; Biron et al. 1990). The pulsating characteristic of a microburst event may prolong the period in which hazardous windshear is maintained and add to the difficulty in deciding when a windshear event is truly dissipating.

At least two different processes give rise to the pulsing characteristic commonly observed in microbursts:

Type-1 pulsing: dynamic/thermodynamic pulsing -- requires a continuous source of precipitation and is analogue to thermals rising from a continuous heat source. As a steady source of precipitation is fed into a microburst downdraft, the precipitation, negative buoyancy, and vertical velocity tends to breakdown into surges or pulses. As will be shown from the results of the model simulation, this case study is an example of type-1 pulsing.

Type-2 pulsing: significant amounts of precipitation accumulates within multiple regions or pockets during the lifetime of the parent storm system, and as each pocket falls a new microburst pulse is initiated. There are at least two ways that type-2 pulsing can occur. In **type-2a pulsing** the accumulation zones are created by multicellular storm updrafts. The Claycomo, Missouri microburst event as described in Biron et al. (1990) is one possible example of this type pulsing. In **type-2b pulsing** multiple regions of precipitation growth/accumulation occur due to precipitation type. For example, a single updraft may produce multiple regions of precipitation accumulation, with rain accumulating in a lower region due collectional growth, and hail/graupel or snow accumulating in higher region. An example of type-2b pulsing is the 20 June 1991, Orlando Microburst as modeled in Proctor (1992). In this case study, the parent storm was characterized by a short-lived single-cell updraft, with two primary accumulation zones for precipitation. The first microburst pulse was initiated by rain falling from the lower zone where precipitation had increased primarily due to collectional growth. Several minutes later, a stronger, second pulse followed, which originated from the higher zone where graupel had accumulated.

3. DOMAIN CONFIGURATION AND INITIAL CONDITIONS

The physical domain size is horizontally: 16 km x 16 km, resolved with a 160 m grid size; and vertically: 13 km deep, resolved with 61 levels having a vertical

spacing stretching from 70 m to 365 m. The environmental condition for the numerical simulation (Fig. 1) was observed less than an hour after the development of the storm and is characteristic of that which produce dry microbursts (e.g., Wakimoto 1985). Development of the parent storm and ensuing microbursts is triggered in the simulation by an initial spheroidal thermal impulse with: a peak amplitude of 1.5° C, a diameter of 5 km, and a depth of 2.5 km.

4. RESULTS

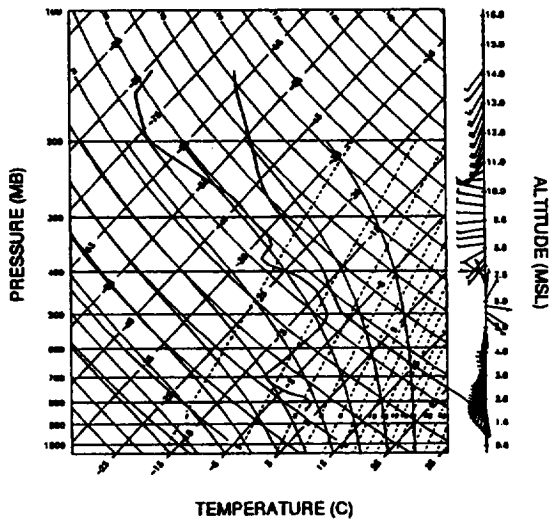

Fig. 1. Input sounding plotted on Skew-T diagram, observed at 0000 UTC, 9 July 1989, Denver. Each full wind barb equals 5 m/s or 10 knots.

The simulation develops a short-lived single-cell updraft with a cloud base ranging between 4 to 4.5 km AGL (at -4° to -8° C). The maximum cloud top of 11 km AGL occurs at 28 min simulation time and precedes the first microburst by 10 min. Precipitation is produced primarily in the form of (graupel-like) snow and is sheared SSE, behind the northward moving storm (Fig. 2). A sub-cloudbase downdraft is initiated at the leading (northward) edge of the cloud following the demise of the storm updraft. The appearance and structure the storm (cf. Figs. 2-4) is similar to the "anteater" cloud described in Fujita (1985). Once the updraft dissipates (at 28 min simulation time), the cloud is nearly stationary.

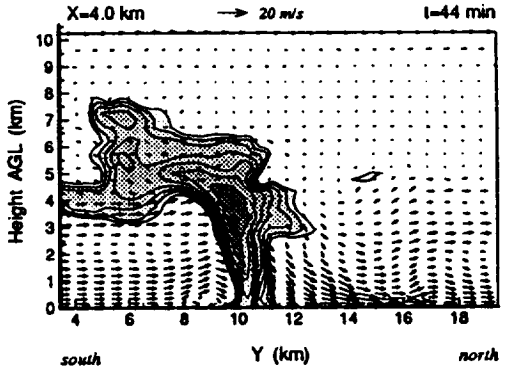

Fig. 3. Vertical N-S cross section of radar reflectivity and wind vectors at 44 min. Contour interval is 5 dBZ starting with -5 dBZ.

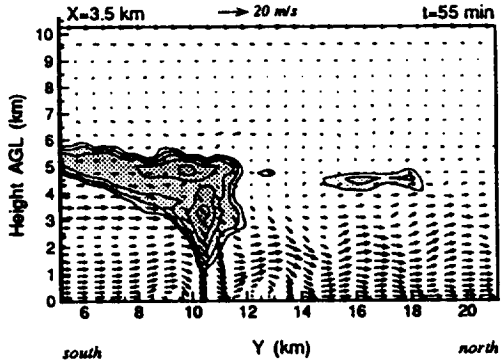

Fig. 4. Same as Fig. 3, but at 55 min.

The first microburst begins about 10 min following the decay of the storm updraft, and windshear from the pulsating microbursts persists for at least 17 min. Inflow into the top of the downdraft (near cloud-base level) pulls in existing cloud material (predominantly snow) and maintains the downdraft with type-1 pulsing (see Figs. 3 and 4). As shown in Proctor (1989) cooling from sublimating snow can drive intense microbursts within typical dry-microburst environments.

The maximum horizontal velocity differential (ΔV) is compared in Fig. 5 for TASS North-South segments

Fig. 2. Three-dimensional perspective of storm viewed from southwest at 5 min intervals starting with 35 min. Isosurface encloses radar reflectivity greater than 0 dBZ.

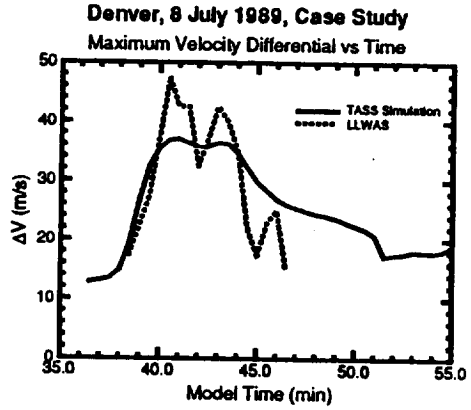

Fig. 5. Comparison of maximum horizontal velocity differential vs time for LLWAS data and TASS simulation. (LLWAS winds from Wilson et al. 1991)

and LLWAS deduced winds. [The LLWAS ΔV is not directly measured but is estimated by fitting the measured winds with a mathematical symmetric-microburst model (Wilson et al. 1991).] The first two of the three pulses detected by LLWAS are in phase with the TASS data, although somewhat more intense. The peak ΔV from the TASS simulation was 38 m/s and occurred along a North-South segment during the first microburst pulse. The TASS simulated peak ΔV along East-West segments is shown in Fig. 6, along with East-West F-factor and peak low-level radar reflectivity. [The 1-km averaged F-factor (Fbar) is computed as described in Proctor and Bowles (1992) and Switzer et al. (1993), and assumes an air speed of 75 m/s. Values of Fbar greater than .105 indicate a hazardous level of aircraft performance loss due to the combined effects of horizontal wind shear and vertical velocity.] The East-West Fbar and ΔV show three pronounced peaks with the strongest values occurring for the second pulse, rather than the first as for the N-S ΔV. The low-level radar reflectivity reaches a maximum of 22 dBZ, 30 s before the first peak in Fbar, and 2.5 min before the first peak in ΔV. The trends of Fbar and low-level radar reflectivity appear roughly correlated, at least until the radar reflectivity drops to less than 0 dBZ after 46 min. After 47 min, ΔV remains above microburst threshold (i.e. 10 m/s) and E-W Fbar remains above hazard threshold (except for a 1 min period), even though precipitation is no longer reaching the ground.

Figs. 7 and 8 show the low-level wind vector field associated with the microburst at the time of the second and third pulse, respectively. The surface-level radar reflectivity (not shown) at the time of Fig. 7 has a peak value of 12 dBZ, with values greater than 0 dBZ limited to within 1 km radius of the divergence center. Most of the outflow is void of precipitation. At the time of Fig. 8 there is no contribution to surface-level radar reflectivity from precipitation. The third pulse is evident in Fig. 8, as a small embedded divergence area near the southern end of the macroburst outflow.

Figs. 3 and 4 show the vertical cross-section of radar reflectivity and wind vectors at the same two times as shown in Figs. 7 and 8. Note that winds above cloud-base level, where most of the precipitation resides, have a relatively weak N-S component. The momentum from the strong southerly flow at sub-cloud-base levels is advected downward by the microburst downdraft and causes the outflow to spread most rapidly toward the north. The southern edge of the outflow remains nearly stationary, as is consistent with observations. Wilson et al. (1991) reported that during the event a line of blowing dust located just north of the north-south runways did not move (southward) toward the airport.

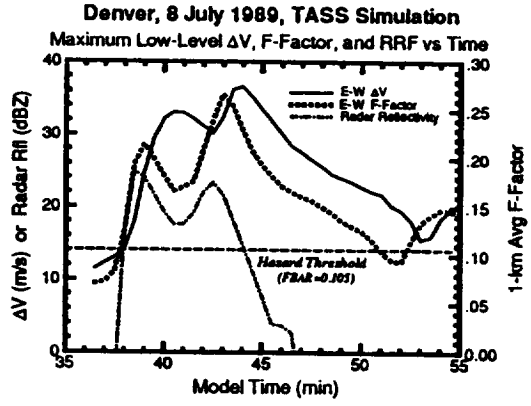

Fig. 6. Low-level maximum vs time for E-W horizontal velocity differential, radar reflectivity factor and E-W 1-km averaged F-factor (Fbar).

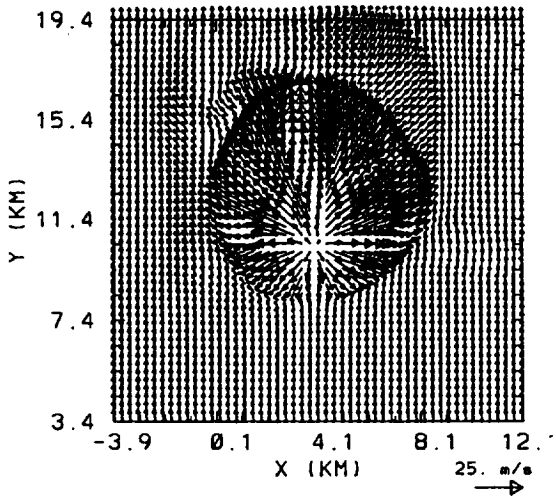

Fig. 7. Low-level horizontal wind vectors at 44 min. North is in the direction of the y coordinate.

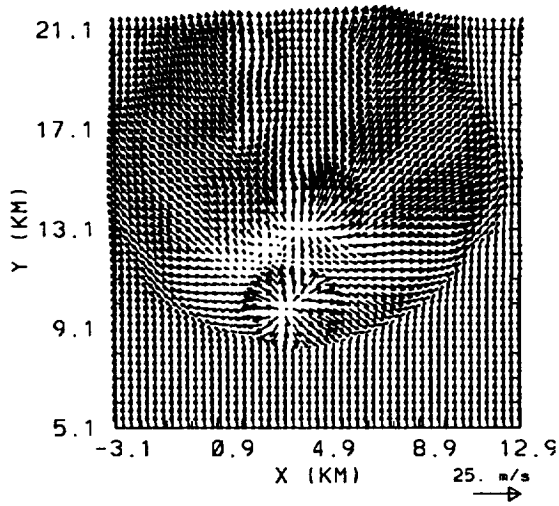

Fig. 8. Same as Fig. 7, but at 55 min.

5. SUMMARY AND CONCLUSIONS

An intense, low-reflectivity, and pulsating microburst event is simulated with a three-dimensional cloud model. The simulation shows that the dissipating cloud induces a type-1 pulsating microburst event, with at least three distinct microburst pulses over a period of 20 min. Virga from the dissipating cloud continued to maintain hazardous windshear for a period much longer than the typical lifetime of a single microburst. Precipitation and radar reflectivity (due to precipitation) occurred aloft; but at the surface, occurred only within a small area around the divergence center, and only then during the first several minutes of the microburst event. Most of the surface outflow contained no precipitation. Such an event may be difficult to detect by radar.

REFERENCES

Biron, P. J., M. A. Isaminger, K. J. Flemming, and A. A. Borho, 1990: A case study of the Claycomo, Mo. microburst on July 30, 1989. Preprints, 16th Conf. on Severe Local Storms, Alberta, Amer. Meteor. Soc., 388-392.

Comman, L. C., P. C. Kucera, M. R. Hjelmfelt, and K. L. Elmore, 1989: Short time-scale fluctuations in microburst outflows as observed by Doppler radars and anemometers. Preprints, 24th Conf. on Radar Meteorology, Tallahassee, Amer. Meteor. Soc., 150-153.

Fujita, T. T., 1985: The Downburst, Microburst, and Macroburst. University of Chicago Press, 122 pp.

Hjelmfelt, M. R., 1988: Structure and life cycle of microburst outflows observed in Colorado. J. Climate Appl. Meteor., 27, 900-927.

Hughes, D., 1990: LLWAS credited with helping 737 survive major microburst. Aviation Week & Space Technology, 133, July-16, pgs. 91, & 93.

Proctor, F. H., 1987: The Terminal Area Simulation System, Volume I: Theoretical formulation. NASA Contractor Rep. 4046, NASA, Washington, DC, 176 pp. [Available from the National Technical Information Service.]

_____, 1988: Numerical simulation of the 2 August 1985 DFW microburst with the three-dimensional Terminal Area Simulation System. Preprints, Joint Session of 15th Conf. on Severe Local Storms and Eighth Conf. on Numerical Weather Pred., Baltimore, Amer. Meteor. Soc., J99-J102.

_____, 1989: Numerical simulations of an isolated microburst. Part II: Sensitivity experiments. J. Atmos. Sci., 46, 2143-2165.

_____, 1992: Three-dimensional numerical simulation of the 20 June 1991, Orlando Microburst. Fourth Combined Manufacturers' and Technologists' Airborne Wind Shear Review Meeting, Williamsburg, VA, 214-242. [Available from the National Technical Information Service.]

_____, and R. L. Bowles, 1992: Three-dimensional simulation of the Denver 11 July 1988 microburst-producing storm. Meteorol. and Atmos. Phys., 47., 107-124.

Switzer, G. F., F. H. Proctor, D. A. Hinton, and J. V. Aanstoos, 1993: Windshear database for forward-looking systems certification. NASA Tech. Mem., 132 pp.

Wakimoto, R. M., 1985: Forecasting dry microburst activity over the High Plains. Mon. Wea. Rev., 113, 1131-1143.

Wilson, F. W., Jr., R. C. Goff, and R. H. Gramzow, 1991: An intense microburst at Denver's Stapleton International Airport. Preprints, Fourth Intl. Conf. on the Aviation Weather System, Paris, Amer. Meteor. Soc.